UMR 5131 CNRS

INTERNATIONAL FEDERATION OF AUTOMATIC CONTROL

1st IFAC Workshop on

# FRACTIONAL DIFFERENTIATION and its APPLICATIONS

## FDA'04

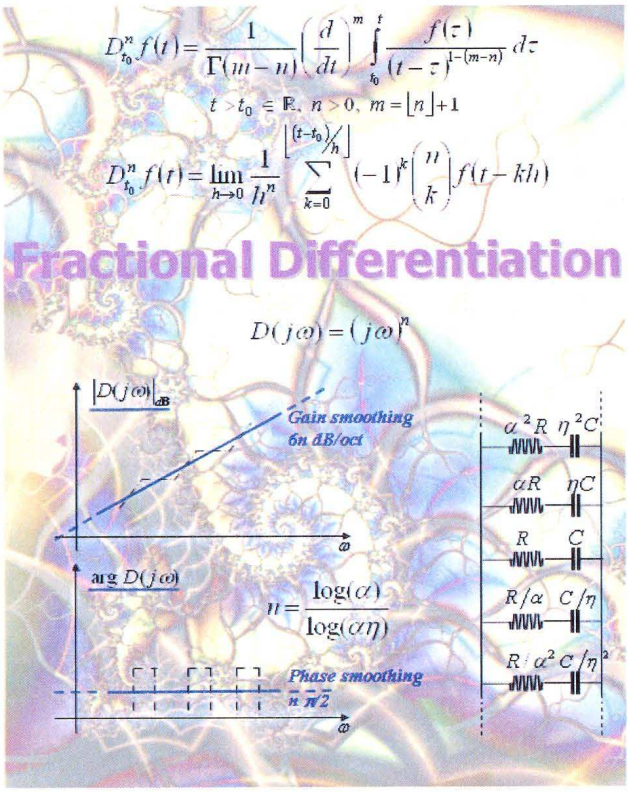


**ENSEIRB, Bordeaux, France, July 19-21, 2004**

## WORKSHOP PREPRINTS/PROCEEDINGS N° 2004-1

UNIVERSITE BORDEAUX 1 Sciences Technologies

CNRS

ENSEIRB ECOLE NATIONALE SUPERIEURE ELECTRONIQUE, INFORMATIQUE & RADIOCOMMUNICATIONS BORDEAUX

# FRACTIONAL-ORDER POSITION/FORCE ROBOT CONTROL

**N. M. Fonseca Ferreira[1], J. A. Tenreiro Machado[2]**
**Alexandra M. Galhano[2], J. Boaventura Cunha[3]**

[1]*Institute of Engineering of Coimbra, Portugal, email: nunomig@isec.pt*
[2]I*nstitute of Engineering of Porto, Portugal, email: jtm@dee.isep.ipp.pt*
[3]*University of Trás dos Montes e Alto Douro, Vila Real, Portugal, email: jboavent@utad.pt*

Abstract: In this paper it is studied the implementation of fractional-order algorithms in the position/force control of two cooperating robotic manipulators. The performance and system robustness are analyzed in the time and frequency domains. The effect of backlash and flexibility at the robot joints is also investigated. *Copyright © 2004 IFAC*

Keywords: Robots, cooperation, position, force, control.

## 1. INTRODUCTION

Two robots carrying a common object are a logical alternative for the case in which a single robot is not able to handle the load. Nevertheless, with two cooperative robots the resulting interaction forces have to be accommodated and consequently, in addition to position feedback, force control is also required (Hogan, 1985 and Siciliano, 1999).

There are two basic methods for force control, namely the hybrid position/force and the impedance schemes. The first method (Raibert and Craig, 1981) requires the separation of the task into two orthogonal subspaces corresponding to the force and the position controlled variables. Once established the subspace decomposition two independent controllers are designed. The second method (Hogan, 1985) requires a proper choice of the arm mechanical impedance through which the interaction forces are indirectly controlled to obtain an adequate response.

This paper studies the position/force control of two cooperative manipulators, using fractional-order (*FO*) algorithms (Oustaloup, 1995, Podlubny, 1999, Ferreira and Machado, 2003). In fact, the application of the fractional calculus is still in a research stage, but the preliminary results reveal properties that can be of importance in the scope of robotic control.

In this line of thought the paper is organized as follows. Section two presents the controller architecture for the position/force control of two robotic arms and section three introduces the fundamentals of the fractional-order algorithms based on these concepts. Section four develops several experiments for the analysis and the performance evaluation of *FO* and the *PID* controllers, for robots having several types of dynamic phenomena at the joints. Finally, section five outlines the main conclusions.

## 2. POSITION-FORCE CONTROL OF TWO ARMS

When two robots grasp an object (Fig. 1), and move it from one location to another, a coordinated motion is required. In order to get good performances it is necessary to specify no only the desired motion of each robot but also the corresponding handling force.

In the system under study the contact of the robot gripper with the load is modeled through a linear system with a mass $M$, a damping $B$ and a stiffness $K$. On the other hand, the dynamics of a robot with $n$ links interacting with the environment is modeled as:

$$\boldsymbol{\tau} = \mathbf{H}(\mathbf{q})\ddot{\mathbf{q}} + \mathbf{C}(\mathbf{q},\dot{\mathbf{q}}) + \mathbf{G}(\mathbf{q}) - \mathbf{J}^{\mathbf{T}}(\mathbf{q})\mathbf{F} \qquad (1)$$

where $\boldsymbol{\tau}$ is the $n \times 1$ vector of actuator torques, $\mathbf{q}$ is the $n \times 1$ vector of joint coordinates, $\mathbf{H(q)}$ is the $n \times n$

inertia matrix, $\mathbf{C(q,\dot{q})}$ is the $n \times 1$ vector of centrifugal/Coriolis terms, $\mathbf{G(q)}$ is the $n \times 1$ vector of gravitational effects, $\mathbf{J^T(q)}$ is the transpose of the Jacobian matrix and $\mathbf{F}$ is the force that the load exerts in the robot gripper.

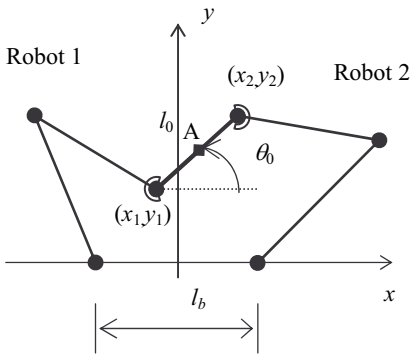


Fig. 1. Two 2*R* cooperating robots for the manipulation of an object with length $l_0$, orientation $\theta_0$ and center point A.

We consider 2*R* manipulators (*i.e.*, $n = 2$) with dynamics:

$$\mathbf{H(q)} = \begin{bmatrix} m_1 + m_2 r_1^2 + m_2 r_2^2 + 2m_2 r_1 r_2 C_2 + J_{1m} + J_{1g} & m_2 r_2^2 + m_2 r_1 r_2 C_2 \\ m_2 r_2^2 + m_2 r_1 r_2 C_2 & m_2 r_2^2 + J_{2m} + J_{2g} \end{bmatrix} \quad (2a)$$

$$\mathbf{C(q,\dot{q})} = \begin{bmatrix} -m_2 r_1 r_2 S_2 \dot{q}_2^2 - 2m_2 r_1 r_2 S_2 \dot{q}_1 \dot{q}_2 \\ m_2 r_1 r_2 S_2 \dot{q}_1^2 \end{bmatrix} \quad (2b)$$

$$\mathbf{G(q)} = \begin{bmatrix} g(m_1 r_1 C_1 + m_2 r_1 C_1 + m_2 r_2 C_{12} \\ g m_2 r_2 C_{12} \end{bmatrix} \quad (2c)$$

$$\mathbf{J^T(q)} = \begin{bmatrix} -r_1 S_1 - r_2 S_{12} & r_1 C_{11} + r_2 C_{12} \\ -r_2 S_{12} & r_2 C_{12} \end{bmatrix} \quad (2d)$$

where $C_{ij} = \cos(q_i + q_j)$ and $S_{ij} = \sin(q_i + q_j)$.

The numerical values adopted for the 2*R* robots and the object are $m_1 = 0.5\ kg$, $m_2 = 6.25\ kg$, $r_1 = 1.0\ m$, $r_2 = 0.8\ m$, $J_{1m} = J_{2m} = 1.0 kgm^2$, $J_{1g} = J_{2g} = 4.0\ kgm^2$ $l_b = l_0 = 1.0\ m$ and $\theta_0 = 0$, $B_1 = B_2 = 1\ Ns.m^{-1}$, $K_1 = K_2 = 10^3\ Nm^{-1}$ and A ≡ {0,1}.

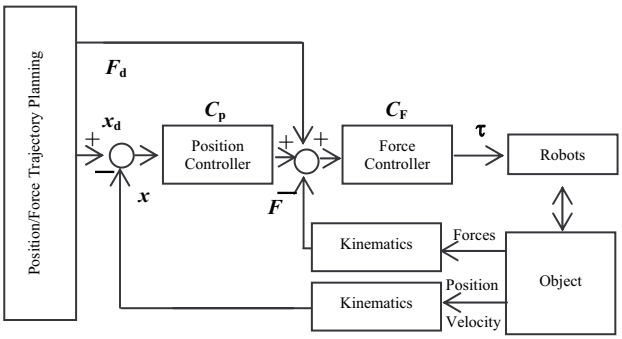


Fig. 2. The position/force controller.

The controller architecture (Fig. 2) is inspired on the impedance and compliance schemes. Therefore, we establish a cascade of force and position algorithms as internal an external feedback loops, respectively, where $\boldsymbol{x}_\mathbf{d}$ and $\boldsymbol{F}_\mathbf{d}$ are the payload desired position coordinates and contact forces.

## 3. FRACTIONAL ORDER ALGORITHMS

In this section we present the *FO* controllers in the position and force control loops.

The mathematical definition of a derivative of fractional order α has been the subject of several different approaches. For example, we can mention the Laplace and the Grünwald-Letnikov definitions:

$$D^\alpha[x(t)] = L^{-1}\{s^\alpha X(s)\} \quad (3a)$$

$$D^\alpha x(t) = \lim_{h \to 0} \frac{1}{h^\alpha} \sum_{k=1}^{\infty} \frac{(-1)^k \Gamma(\alpha+1)}{\Gamma(k+1)\,\Gamma(\alpha-k+1)} x(t-kh) \quad (3b)$$

where Γ is the gamma function and $h$ is the time increment.

In this article we consider *FO* controllers of the type:

$$C(s) = K_0 + K_\alpha s^\alpha,\ -1 < \alpha < 1 \quad (5)$$

For implementing (5) we adopt discrete-time $k = 4$ Padé approximations ($K$, $a_i$, $b_i \in \Re$):

$$C(z) \approx K \sum_{i=0}^{k} a_i z^i \Big/ \sum_{i=0}^{k} b_i z^i \quad (6)$$

both in the position (P) and force (F) loops.

## 4. CONTROLLER PERFORMANCES

This section analyzes the system performance both for robots ideal transmissions and robots with dynamic phenomena at the joints, such as backlash and flexibility. Moreover, we compare the response of *FO* and classical *PID* algorithms. In particular we adopt a *PD* and a *PI* in the position (P) and force (F) loops, respectively:

Position-*PD* algorithm: $C(s) = K_p + K_d\, s$ (7a)

Force-*PI* algorithm: $C(s) = K_p + K_i\, s^{-1}$ (7b)

Both algorithms were tuned by trial and error having in mind getting a similar performance in the two cases. By other words, the parameters were adjusted not only to get small overshoots and steady-state errors, but also to have similar performances in the *FO* and *PID* schemes in order to easy their comparison.

The resulting parameters were $\{K_0, K_\alpha, \alpha\}_P \equiv \{7.9\ 10^4, 190, 0.5\}$, $\{K_0, K_\alpha, \alpha\}_F \equiv \{10.4, 179, -0.2\}$ for the *FO* and $\{K_p, K_d\}_P \equiv \{10^4, 10^2\}$, $\{K_p, K_i\}_F \equiv \{10, 10^4\}$ for the *PD*/*PI*, in the position and force loops, respectively.

In order to study the system dynamics we apply, separately, small amplitude rectangular pulses, at the position and force reference, that is, we perturb each

reference signal at a time with $\delta x_d = 10^{-3}$ m, $\delta y_d = 10^{-3}$ m, $\delta Fx_d = 1.0$ N and $\delta Fy_d = 1.0$ N. Afterward, we analyze the system performance both in the time and the frequency domains.

*4.1 Time response*

In order to evaluate the performance of the proposed algorithms we compare the response for robots with dynamical phenomena at the joints.

In all experiments the controller sampling frequency is $f_c = 10$ kHz for the operating point A of the object and a contact force of each gripper of $\{Fx_j, Fy_j\} \equiv \{0.5, 5\}$ *Nm* for the *j*th ($j = 1, 2$) robot.

In a first phase we consider robots with ideal transmissions at the joints. Figures 3 and 4 depict the time response of the robots 1 and 2, under the action of the *FO* and the *PD/PI* algorithms.

In a second phase (Fig. 5) we analyze the response of robots with dynamic backlash at the joints (Stepanenko, 1986, and Dubowsky, 1987). For the *i*th joint gear, with clearance $h_i$, the backlash reveals impact phenomena between the inertias, which obey the principle of conservation of momentum and the Newton law:

$$\dot{q}_i' = \frac{\dot{q}_i (J_{ii} - \varepsilon J_{im}) + \dot{q}_{im} J_{im} (1 + \varepsilon)}{J_{ii} + J_{im}} \qquad (8a)$$

$$\dot{q}_{im}' = \frac{\dot{q}_i J_i (1 + \varepsilon) + \dot{q}_{im} (J_{im} - \varepsilon J_{ii})}{J_{ii} + J_{im}} \qquad (8b)$$

where $0 \le \varepsilon \le 1$ is a constant that defines the type of impact ($\varepsilon = 0$ inelastic impact, $\varepsilon = 1$ elastic impact) and $\dot{q}_i'$ and $\dot{q}_{im}'$ are the inertias velocities of the *i*th joint and motor after the collision, respectively. The parameter $J_{ii}$ ($J_{im}$) stands for the link (motor) inertias of joint *i*. The numerical values adopted are $h_i = 1.8\ 10^{-4}$ rad and $\varepsilon_i = 0.8$ ($i = 1, 2$).

In a third phase (Fig. 6) we study the performance of robots with compliant joints. For this case the dynamic model corresponds to model (1) augmented by the equations:

$$\boldsymbol{\tau} = \mathbf{J_m}\ddot{\mathbf{q}}_\mathbf{m} + \mathbf{B_m}\dot{\mathbf{q}}_\mathbf{m} + \mathbf{K_m}(\mathbf{q_m} - \mathbf{q}) \qquad (9a)$$

$$\mathbf{K_m}(\mathbf{q_m} - \mathbf{q}) = \mathbf{J}(\mathbf{q})\ddot{\mathbf{q}} + \mathbf{C}(\mathbf{q}, \dot{\mathbf{q}})\dot{\mathbf{q}} + \mathbf{G}(\mathbf{q}) \qquad (9b)$$

where $\mathbf{J_m}$, $\mathbf{B_m}$ and $\mathbf{K_m}$ are the $n \times n$ diagonal matrices of the motor and transmission inertias, damping and stiffness, respectively. In the simulations we adopt $K_{mi} = 2\ 10^6$ Nm rad$^{-1}$ and $B_{mi} = 10^4$ Nms rad$^{-1}$ ($i = 1,2$).

The time responses (Tables 1 to 4), namely the percent overshoot *PO%*, the steady-state error $e_{ss}$, the peak time $T_p$ and the settling time $T_s$, reveal that, although tuned for similar performances in the first case, the *FO* is superior to the *PD/PI* in the cases with dynamical phenomena at the robot joints.

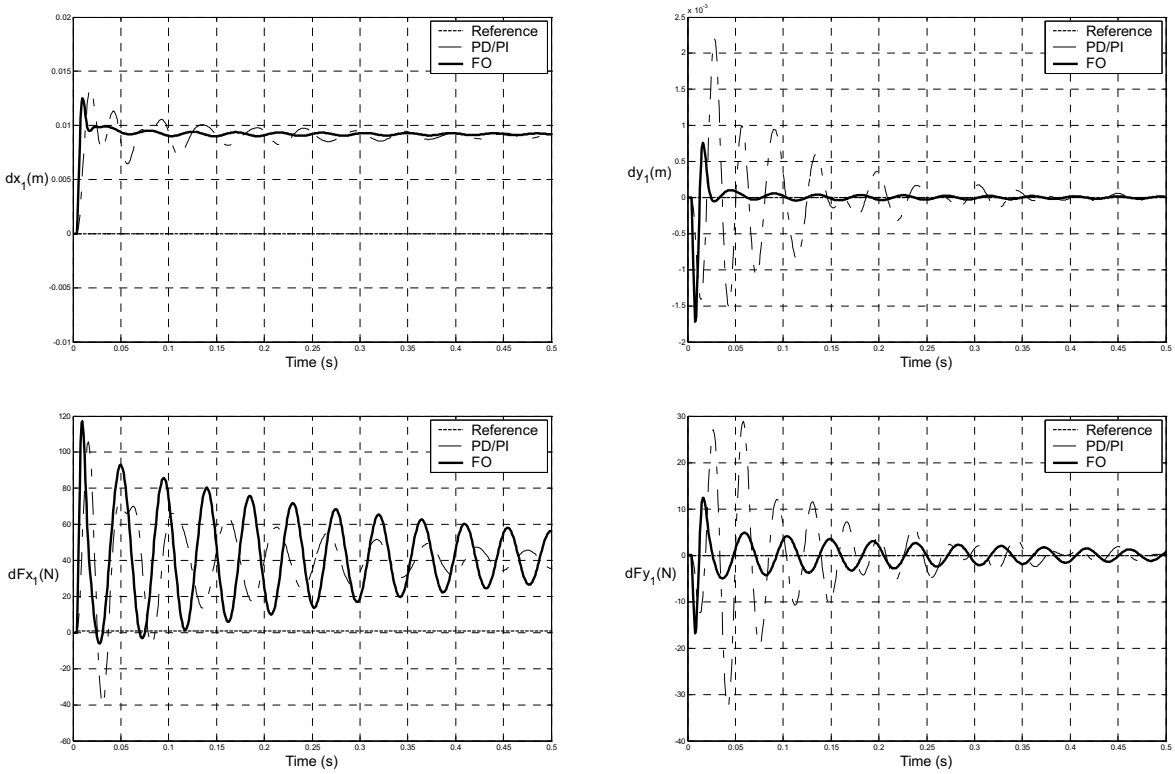


Fig. 3. Time response for the robot 1 under the action of the *FO* and the *PD/PI* algorithms, for a pulse perturbation $\delta x_d = 10^{-3}$m at the robot 1 position reference.

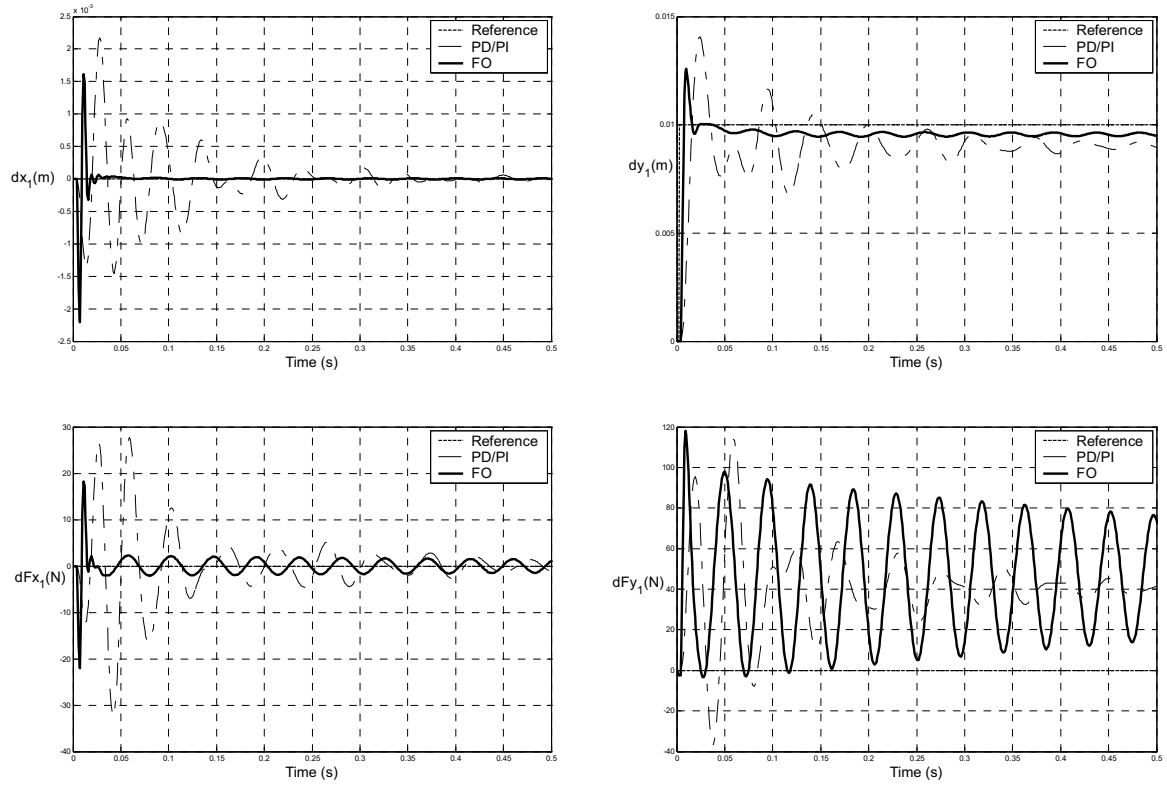


Fig. 4. Time response for the robot 1 under the action of the *FO* and the *PD/PI* algorithms for a pulse perturbation $\delta y_d = 10^{-3}$m at the robot 1 position reference.

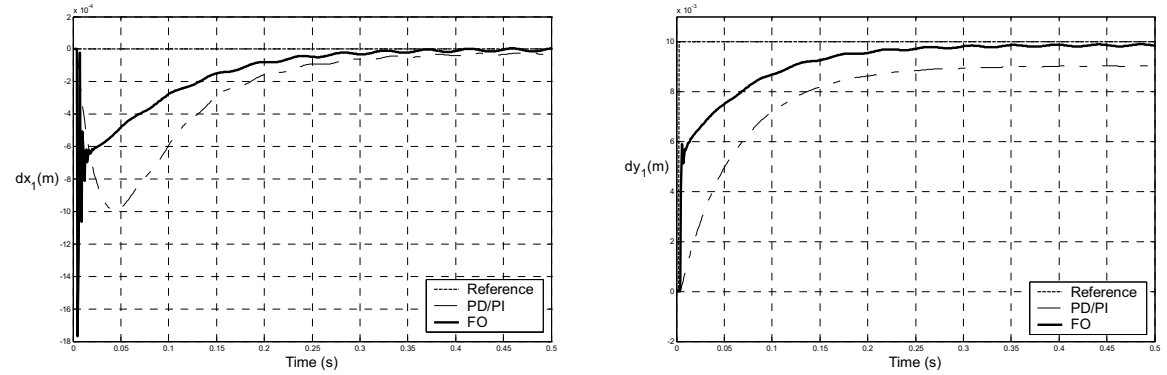


Fig. 5. Time response for the robot 1 with joints having backlash under the action of the *FO* and *PD/PI* algorithms for a pulse perturbation $\delta y_d = 10^{-3}$m at the robot 1 position reference.

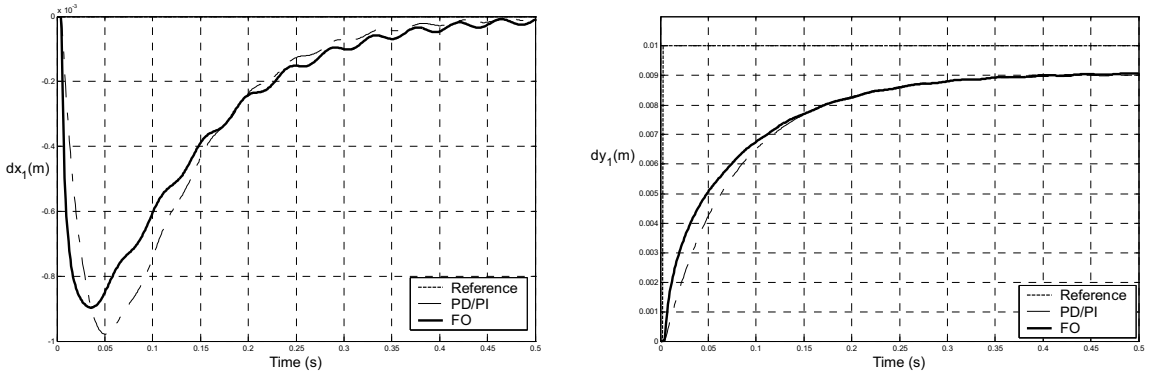


Fig. 6. Time response for the robot 1 with joints having flexibility under the action of the *FO* and *PD/PI* algorithms for a pulse perturbation $\delta y_d = 10^{-3}$m at the robot 1 position reference.

Table 1 Parameters of the time response for a rectangular pulse $\delta x_d$ the robot 1 position reference.

| Joint | $C(s)$ | $PO\%$ | $e_{ss}$ | $T_p$ | $T_s$ |
|---|---|---|---|---|---|
| Ideal | *PID* | 33.75 | $3.4\ 10^{-3}$ | $17\ 10^{-3}$ | $65\ 10^{-2}$ |
| | *FO* | 33.70 | $2.5\ 10^{-3}$ | $9\ 10^{-3}$ | $25\ 10^{-2}$ |
| Backlash | *PID* | 0.84 | $0.5\ 10^{-3}$ | $20\ 10^{-3}$ | $20\ 10^{-3}$ |
| | *FO* | 1.23 | $0.2\ 10^{-3}$ | $25\ 10^{-3}$ | $25\ 10^{-3}$ |
| Flexible | *PID* | 0.54 | $0.5\ 10^{-2}$ | $10\ 10^{-3}$ | $20\ 10^{-3}$ |
| | *FO* | 0.37 | $1.0\ 10^{-3}$ | $25\ 10^{-3}$ | $25\ 10^{-2}$ |

Table 2 Time response parameters for rectangular pulse $\delta y_d$ the robot 1 position reference.

| Joint | $C(s)$ | $PO\%$ | $e_{ss}$ | $T_p$ | $T_s$ |
|---|---|---|---|---|---|
| Ideal | *PID* | 30.36 | $4.1\ 10^{-4}$ | $23\ 10^{-3}$ | $70\ 10^{-2}$ |
| | *FO* | 30.61 | $2.6\ 10^{-4}$ | $9\ 10^{-3}$ | $50\ 10^{-2}$ |
| Backlash | *PID* | 0.11 | $1.2\ 10^{-3}$ | $30\ 10^{-3}$ | $40\ 10^{-3}$ |
| | *FO* | 0.82 | $0.2\ 10^{-4}$ | $30\ 10^{-3}$ | $40\ 10^{-3}$ |
| Flexible | *PID* | 0.11 | $0.9\ 10^{-2}$ | $40\ 10^{-3}$ | $45\ 10^{-3}$ |
| | *FO* | 0.20 | $0.9\ 10^{-3}$ | $40\ 10^{-3}$ | $45\ 10^{-2}$ |

Table 3 Time response parameters for rectangular pulse $\delta Fx_d$ at the robot 1 force reference.

| Joint | $C(s)$ | $PO\%$ | $e_{ss}$ | $T_p$ | $T_s$ |
|---|---|---|---|---|---|
| Ideal | *PID* | 36.5 | $9.2\ 10^{-3}$ | $15\ 10^{-3}$ | $75\ 10^{-2}$ |
| | *FO* | 36.5 | $8.4\ 10^{-3}$ | $58\ 10^{-3}$ | $55\ 10^{-2}$ |
| Backlash | *PID* | 13.3 | $9.2\ 10^{-3}$ | $14\ 10^{-2}$ | $50\ 10^{-2}$ |
| | *FO* | 7.5 | $9.2\ 10^{-3}$ | $28\ 10^{-2}$ | $50\ 10^{-2}$ |
| Flexible | *PID* | 13.3 | $9.2\ 10^{-3}$ | $14\ 10^{-2}$ | $50\ 10^{-2}$ |
| | *FO* | 7.5 | $9.2\ 10^{-3}$ | $28\ 10^{-2}$ | $50\ 10^{-2}$ |

Table 4 Time response parameters for rectangular pulse $\delta Fy_d$ at the robot 1 force reference.

| Joint | $C(s)$ | $PO\%$ | $e_{ss}$ | $T_p$ | $T_s$ |
|---|---|---|---|---|---|
| Ideal | *PID* | 58.1 | $9.2\ 10^{-4}$ | $15\ 10^{-3}$ | $75\ 10^{-2}$ |
| | *FO* | 51.3 | $8.4\ 10^{-4}$ | $58\ 10^{-3}$ | $55\ 10^{-2}$ |
| Backlash | *PID* | 52.3 | $9.2\ 10^{-4}$ | $55\ 10^{-2}$ | $60\ 10^{-2}$ |
| | *FO* | 6.6 | $9.2\ 10^{-4}$ | $5\ 10^{-2}$ | $60\ 10^{-2}$ |
| Flexible | *PID* | 52.3 | $9.2\ 10^{-4}$ | $55\ 10^{-2}$ | $60\ 10^{-2}$ |
| | *FO* | 6.6 | $9.0\ 10^{-4}$ | $5\ 10^{-2}$ | $60\ 10^{-2}$ |

*4.2. Frequency response*

In order to compare the robustness of the algorithm, we analyze the system response for ideal robots and robots having flexible transmission.

Based on the time response to small perturbations at the position and force references we can establish the frequency response, corresponding to linearized transfer functions around the operating point A.

Figures 7-8 show the closed-loop transfer functions $|X(j\omega)/X_d(j\omega)|$, $|Y(j\omega)/Y_d(j\omega)|$, $|Fx(j\omega)/Fx_d(j\omega)|$ and $|Fy(j\omega)/Fy_d(j\omega)|$ (where $X(j\omega)=F\{\delta x\}$, $Y(j\omega)=F\{\delta y\}$, where $Fx(j\omega)=F\{\delta Fx\}$ and $Fy(j\omega)=F\{\delta Fy\}$) for the *FO* and the *PD*/*PI* controllers, in both cases.

The charts reveal that the *FO* algorithms have a superior performance, namely a good robustness and larger bandwidth.

## 5. SUMMARY AND CONCLUSIONS

This paper compared the position/force control of two robots working in cooperation using a fractional-order and integer order control algorithms. The dynamic performance of two arms holding an object was analyzed both in the time and the frequency domains and the manipulators were also tested for several types of nonlinear phenomena at the joints.

The results demonstrate that the fractional-order algorithm is superior, revealing a good performance and a high robustness.

## REFERENCES


Raibert, M. H. and Craig, J. J. (1981). Hybrid Position/Force Control of Manipulators. *ASME J. of Dynamic Systems, Measurement, and Control*" vol. 2, No. 2, pp.126-133, vol. 1.

Hogan, N. (1985). Impedance control: An Approach to Manipulation, Parts I-Theory, II-Implementation, III-Applications. *ASME J. of Dynamic Systems, Measurement and Control*, vol. 107, No. 1, pp. 1-24.

Stepanenko, Y. and Sankar, T. S. (1986), "Vibro-Impact Analysis of Control Systems with Mechanical Clearance and Its Application to Robotic Actuators", *ASME Journal of Dynamic Systems, Measurement and Control*, vol. 108, no. 1, pp. 9–16.

Dubowsky, S. Deck, J. F. and Costello, H. (1987). The Dynamic Modelling of Flexible Spatial Machine Systems with Clearance Connections. *ASME Journal of Mechanisms, Transmissions and Automation in Design,* vol. 109, no. 1, pp. 87–94.

Oustaloup, A. (1995). *La Dérivation Non Entière: Théorie, Synthèse et Applications*, Hermes, Paris.

Tenreiro Machado, J. (1997). Analysis and Design of Fractional-Order Digital Control Systems. *J. Systems Analysis, Modelling and Simulation*, vol. 27, pp. 107–122.

Siciliano, B. and Villani, L. (1999). Robot Force Control. *Kluwer Academic Publishers*.

Podlubny, I. (1999). Fractional-Order Systems and $PI^{\lambda}D^{\mu}$-Controllers. *IEEE Trans. on Automatic Control*, vol. 44, no. 1, pp. 208–213.

Fonseca Ferreira, N. M. and Tenreiro Machado, J. A. (2003). Fractional-Order Hybrid Control of Robotic Manipulator, *Proceedings of the 11th IEEE Int. Conf. on Advanced Robotics, Coimbra, Portugal*.

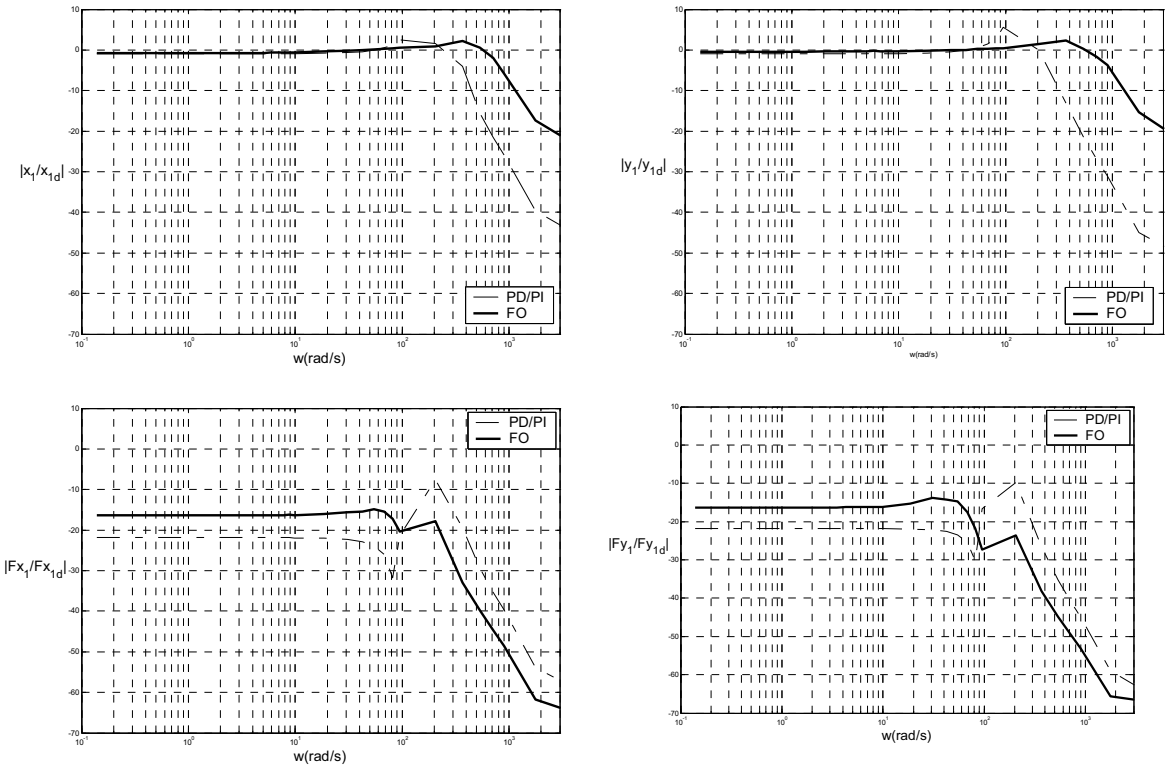


Fig. 7. Closed loop frequency responses for the ideal robot 1, under the action of the *FO* and *PD/PI* algorithm, for pulse perturbations $\delta x_d$, $\delta y_d$, $\delta Fx_d$ and $\delta Fy_d$ at the robot 1 references.

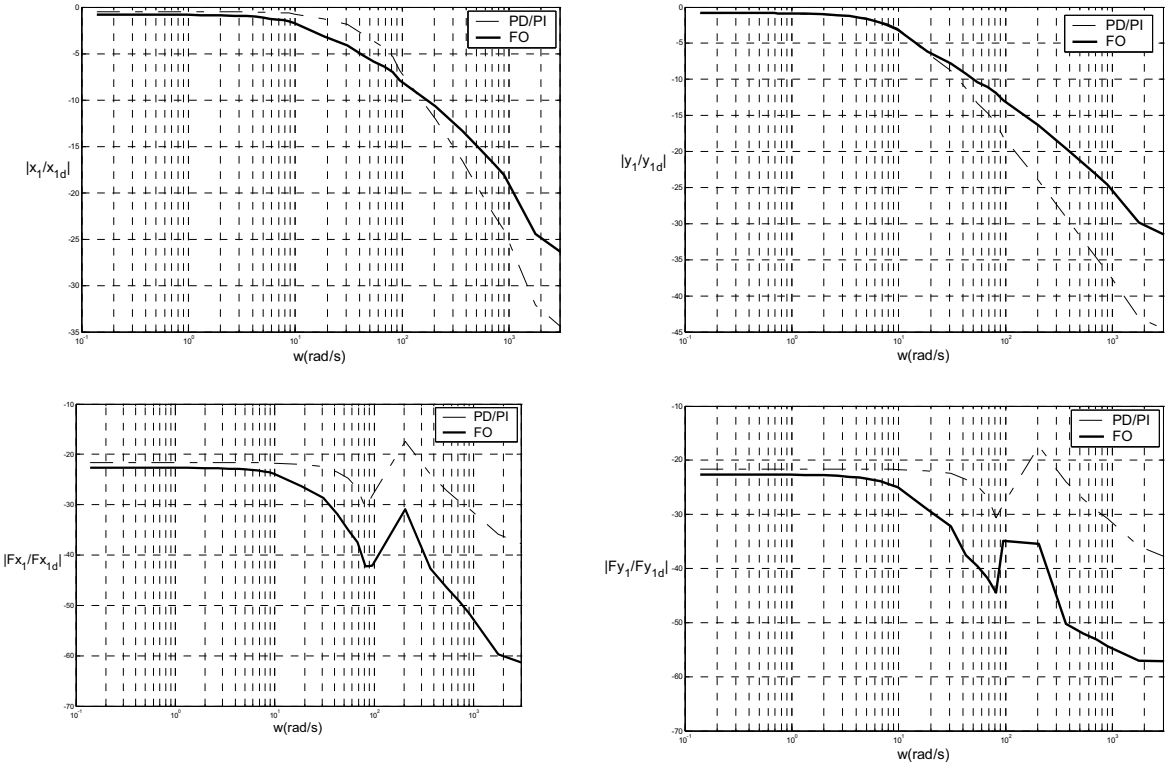


Fig. 8. Closed loop frequency responses for the robot 1 with joints having flexibility, under the action of the *FO* and *PD/PI* algorithm, for pulse perturbations $\delta x_d$, $\delta y_d$, $\delta Fx_d$ and $\delta Fy_d$ at the robot 1 references.